JOURNAL OF GEOPHYSICAL RESEARCH, VOL. 86, NO. B5, PAGES 3951–3959, MAY 10, 1981

Role of Membrane Stresses in the Support of Planetary Topography

D. L. TURCOTTE AND R. J. WILLEMANN

Department of Geological Sciences, Cornell University, Ithaca, New York 14853

W. F. HAXBY

Lamont-Doherty Geological Observatory, Columbia University, Palisades, New York 10964

JOHN NORBERRY

Mathematical Institute, University of Oxford, Oxford, England

The principal purpose of this paper is to examine whether membrane stresses can support topographic loads on planetary elastic lithospheres. It is found that the ability of a spherical shell to support loads through membrane stresses is determined by the nondimensional parameter $\tau = Ed/\Delta\rho gR^2$ where d is the thickness of the elastic lithosphere, $\Delta\rho$ is the density difference between the mantle and crust, and R is the radius of the planetary body. When this parameter is large membrane stresses can fully support topographic loads without flexure, and when it is small the influence of membrane stresses can be neglected. Solutions of the equation governing the behavior of a spherical shell are obtained for a topographic load expressed in terms of spherical harmonics. Spherical harmonic expansions of the measured gravity and topography for Mars and the moon are compared with the theory. It is found that for Mars the support of topography is primarily due to membrane stresses for $n < 8$ and for the moon for $n < 17$. For Mars the data for $4 \le n \le 7$ give $\tau \simeq 0.5$. For the moon the data have considerable scatter that is attributed to the mascons but generally correlate with $\tau = 0.5$. If bending stresses are neglected, the governing equation for the deflection of the spherical shell is Legendre's equation. A general solution is obtained for an axisymmetric load. This solution is applied to the Tharsis region on Mars. The 60–65% compensation of this region requires that $\tau = 0.6$. The well defined fracture pattern surrounding the Tharsis region is attributed to tensional membrane stresses.

INTRODUCTION

It is now widely accepted that planetary bodies have thin, near-surface shells that behave elastically on geological time scales. Beneath the shell, the elastic lithosphere, the mantle behaves as a fluid. Assuming that the spherical shell with radius R has a constant thickness d the equation for the vertical displacement w (measured positive downwards) is [*Kraus*, 1967]

$$D\nabla^6 w + 4D\nabla^4 w + EdR^2\nabla^2 w + 2EdR^2 w = R^4(\nabla^2 + 1 - \nu)p \tag{1}$$

where $D = Ed^3/12(1 - \nu^2)$ is the flexural rigidity, E Young's modulus, ν Poisson's ratio, and p the pressure on the shell (positive directed inwards). The Laplacian operator ∇^2 is defined by

$$\nabla^2 \equiv \frac{\partial^2}{\partial\phi^2} + \cot\phi\,\frac{\partial}{\partial\phi} + \csc^2\phi\,\frac{\partial^2}{\partial\psi^2} \tag{2}$$

with ϕ the polar angle (colatitude) and ψ the azimuthal angle (longitude).

We assume that topography of height h is added onto the shell; the weight of the topography is one contribution to the pressure p. If the shell is not infinitely rigid the weight of the topography will cause a downward displacement of the shell w. This downward displacement will depress the Moho at which there is a density contrast $\rho_m - \rho_c$; the result is an upward (negative) pressure. The additional mass of the topography, however, also causes an upward displacement of the geoid h_g; the pressure contribution of this upward displacement is $-\rho_m h_g$. This latter effect is only important for loads whose wavelengths are of the order of the radius R. The pressure is therefore given by

$$p = g[\rho_c h - \rho_m h_g - (\rho_m - \rho_c)w] \tag{3}$$

In writing the term $-(\rho_m - \rho_c)w$ it is implicitly assumed that crust with density ρ_c fills the region between 0 and w. The height h is the actual height of the topography above the reference sphere of radius R. The actual amount of crustal rock that must be added is $h + w$. For convenience a new variable is introduced

$$\bar{h} = h - \frac{\rho_m}{\rho_c} h_g \tag{4}$$

Our formulation includes both membrane and bending stresses.

For loads which have a wavelength small compared with the radius R it is appropriate to neglect both the curvature and h_g so that (1) to (3) reduce to

$$\frac{1}{R^4} D\nabla^4 + (\rho_m - \rho_c)gw = \rho_c gh \tag{5}$$

Solutions to this equation decrease exponentially in a distance $\alpha = [4D/(\rho_m - \rho_c)g]^{1/4}$ which is the flexural parameter.

Paper number 1B0022.
0148-0227/81/001B-0022$01.00

Topography which has a wavelength small compared with the flexural parameter can be supported by the flexural rigidity of the elastic lithosphere and is not compensated. Topography which has a wavelength large compared with the flexural parameter is not supported and is fully compensated in the flat earth limit. Solutions of (5) as a function of wavelength have been obtained by *Banks et al.* [1977] and were compared with the cross correlation of gravity and topography for the United States given by *Dorman and Lewis* [1972]. A similar correlation for Australia has been given by *McNutt and Parker* [1978] and for Africa by *Banks and Swain* [1978].

In this paper we wish to determine whether some fraction of the topographic load can be supported by the membrane stresses in the elastic lithosphere. If the curvature of the surface is neglected then loading is entirely supported by bending stresses. However, once curvature is introduced the horizontal membrane stresses can support the load.

Harmonic Analysis

In order to study the roles of membrane stresses and bending stresses in supporting topographic loads it is convenient to introduce the dimensionless parameters

$$\tau \equiv \frac{Ed}{R^2 g(\rho_m - \rho_c)} \tag{6}$$

$$\sigma \equiv \frac{D}{R^4 g(\rho_m - \rho_c)} = \frac{\tau}{12(1-\nu^2)}\left(\frac{d}{R}\right)^2 \tag{7}$$

The parameter τ is a measure of the rigidity of the spherical shell if bending resistance is neglected. The parameter σ is a measure of the resistance of the shell to bending. Using these parameters and the variable $\bar{h}$ defined in (4), we rewrite (1) as

$$[\sigma(\nabla^6 + 4\nabla^4) + \tau(\nabla^2 + 2)]w = (\nabla^2 + 1 - \nu)\left(\frac{\rho_c}{\rho_m - \rho_c}\bar{h} - w\right) \tag{8}$$

Our object is to obtain w as a function of $\bar{h}$. In order to do this we expand w and $\bar{h}$ in spherical harmonics

$$\bar{h} = \sum_{n=1}^{\infty}\sum_{m=0}^{n} \bar{h}_{nm} P_{nm}(\cos\phi) \tag{9}$$

$$w = \sum_{n=1}^{\infty}\sum_{m=0}^{n} w_{nm} P_{nm}(\cos\phi) \tag{10}$$

where

$$\bar{h}_{nm} = \bar{h}_{cnm}\cos m\psi + \bar{h}_{snm}\sin m\psi \tag{11}$$

$$w_{nm} = w_{cnm}\cos m\psi + w_{snm}\sin m\psi \tag{12}$$

and P_{nm} are the associated Legendre polynominals of degree n and order m. However, the associated Legrendre polynomials satisfy Legendre's equation so that

$$\left[(1-\xi^2)\frac{\partial^2}{\partial\xi^2} - 2\xi\frac{\partial}{\partial\xi} + \frac{1}{(1-\xi^2)}\frac{\partial^2}{\partial\psi^2} + n(n+1)\right] \cdot P_{nm}(\xi)\cos m\psi = 0 \tag{13}$$

$$\left[(1-\xi^2)\frac{\partial^2}{\partial\xi^2} - 2\xi\frac{\partial}{\partial\xi} + \frac{1}{(1-\xi^2)}\frac{\partial^2}{\partial\psi^2} + n(n+1)\right] \cdot P_{nm}(\xi)\sin m\psi = 0 \tag{14}$$

If we introduce

$$\xi = \cos\phi \tag{15}$$

in spherical coordinates the Laplacian operator is related to Legendre's equation by

$$\nabla^2 = (1-\xi^2)\frac{\partial^2}{\partial\xi^2} - 2\xi\frac{\partial}{\partial\xi} + \frac{1}{(1-\xi^2)}\frac{\partial^2}{\partial\psi^2} \tag{16}$$

using (2) and (15). Combining (13), (14), and (15), we obtain

$$\nabla^2[P_{nm}(\xi)\cos m\psi] = -n(n+1)P_{nm}(\xi)\cos m\psi \tag{17}$$

$$\nabla^2[P_{nm}(\xi)\sin m\psi] = -n(n+1)P_{nm}(\xi)\sin m\psi \tag{18}$$

as long as the Laplacian operator is expressed in spherical polar coordinates.

Substitution of (9), (10), (11), (12), (17) and (18) into (8) gives

$$\{\sigma[-n^3(n+1)^3 + 4n^2(n+1)^2] + \tau[-n(n+1)+2]\}w_{cnm} = [-n(n+1) + (1-\nu)]\left[\frac{\rho_c}{(\rho_m - \rho_c)}\bar{h}_{cnm} - w_{cnm}\right] \tag{19}$$

$$\{\sigma[-n^3(n+1)^3 + 4n^2(n+1)^2] + \tau[-n(n+1)+2]\}w_{snm} = [-n(n+1) + (1-\nu)]\left[\frac{\rho_c}{(\rho_m - \rho_c)}\bar{h}_{snm} - w_{snm}\right] \tag{20}$$

Because the functions $P_{nm}(\cos\phi)\cos m\psi$ and $P_{nm}(\cos\phi)\sin m\psi$ are orthogonal the coefficients of each of these terms in the infinite expansion must be identically equal to zero. From (19) and (20) we find that the ratios of the coefficients are given by

$$\frac{w_{cnm}}{\bar{h}_{cnm}} = \frac{w_{snm}}{\bar{h}_{snm}} = \left(\frac{\rho_c}{\rho_m - \rho_c}\right)\left\{\frac{n(n+1) - (1-\nu)}{\sigma[n^3(n+1)^3 - 4n^2(n+1)^2] + \tau[n(n+1)-2] + n(n+1) - (1-\nu)}\right\} \tag{21}$$

This is a simple algebraic expression for the ratio of the deflection coefficients w_{cnm} and w_{snm} to the loading coefficients $\bar{h}_{cnm}$ and $\bar{h}_{snm}$.

It is now necessary to determine the elevation of the geoid h_g caused by the additional mass of the topography. The gravitational potential at a radial position r of a sphere of mass M with a mass distribution of topography, $\rho_c h$, at the surface $r = R$ and a mass difference due to the deflection of the Moho, $(\rho_m - \rho_c)w$, at a radial position $r = R - b_c$ where b_c is the thickness of the crust is [*Jeffreys*, 1976, 5.06.1]

$$U = -\frac{GM}{r} - 4\pi G\sum_{n=1}^{\infty}\sum_{m=0}^{\infty} \cdot \left[\frac{R^{n+2}\rho_c h_{nm} - (R-b_c)^{n+2}(\rho_m - \rho_c)w_{nm}}{(2n+1)r^{n+1}}\right] P_{nm}(\cos\phi) \tag{22}$$

We expand the radial position of the geoid in terms of spherical harmonics according to

$$r = R + \sum_{n=1}^{\infty} \sum_{m=0}^{n} h_{gnm} P_{nm} (\cos \phi) \tag{23}$$

where h_{gnm} is related to h_{gcnm} and h_{gsnm} as in (11).

The value of the potential on the reference geoid is

$$U = -\frac{GM}{R} \tag{24}$$

We substitute (23) and (24) into (27) and set coefficients of orthogonal functions equal to zero. The elevation of the geoid will be significant only for low degree terms so that is is appropriate to assume $(1 - b_c/R)^{n+2} = 1$ when determining h_{gcnm} and h_{gsnm}. With this approximation and assuming that $h_g/R \ll 1$ we obtain (note that it is appropriate to set $r^{n+1} = R^{n+1}$ to a consistent order within the summations)

$$h_{gcnm} = \frac{3}{(2n+1)\bar{\rho}} [\rho_c h_{cnm} - (\rho_m - \rho_c) w_{cnm}] \tag{25}$$

where $\bar{\rho}$ is the mean density of the planet. An identical result relates h_{gsnm}, h_{snm}, and w_{snm}. Substitution of (4) and (25) into (21) gives

$$\frac{w_{cnm}}{h_{cnm}} = \frac{w_{snm}}{h_{snm}} = \frac{\rho_c}{\rho_m - \rho_c} C_n \tag{26}$$

where

$$C_n = \left\{1 - \frac{3\rho_m}{(2n+1)\bar{\rho}}\right\} \cdot \left\{\frac{\sigma[n^3(n+1)^3 - 4n^2(n+1)^2] + \tau[n(n+1) - 2] + n(n+1) - (1-\nu)}{n(n+1) - (1-\nu)} - \frac{3\rho_m}{(2n+1)\bar{\rho}}\right\}^{-1} \tag{27}$$

We will show that it is appropriate to refer to C_n as the degree of compensation for degree n.

In the limit of a lithosphere with no strength ($\tau \rightarrow 0$, $\sigma \rightarrow 0$) $C_n \rightarrow 1$ and (26) reduces to

$$\left(\frac{w_{cnm}}{h_{cnm}}\right)_0 = \frac{\rho_c}{\rho_m - \rho_c} \tag{28}$$

The load is isostatically compensated. In the limit of a rigid lithosphere ($\tau \rightarrow \infty$, $\sigma \rightarrow \infty$) $C_n \rightarrow 0$ and there is no compensation and no deflection

$$\left(\frac{w_{cnm}}{h_{cnm}}\right)_\infty = 0 \tag{29}$$

Thus C_n as defined in (27) is identically equal to the degree of compensation defined as

$$C_n = \frac{(w_{cnm}/h_{cnm})}{(w_{cnm}/h_{cnm})_0} \tag{30}$$

For short wavelength loads $n(n+1) \gg 1$ (27) reduces to

$$C_n = \frac{1}{1 + \sigma[n^2(n+1)^2]} \tag{31}$$

In this limit bending stresses dominate. This result can also be obtained directly from (5) using (17) or (18) and (26).

For relatively small planetary bodies and small values of n it is appropriate to neglect bending stresses compared with membrane stresses. In this limit, $\sigma \rightarrow 0$, we obtain

$$C_n = \left\{1 - \frac{3\rho_m}{(2n+1)\bar{\rho}}\right\} \cdot \left\{1 - \frac{3\rho_m}{(2n+1)\bar{\rho}} + \tau \left[\frac{n(n+1) - 2}{n(n+1) - (1-\nu)}\right]\right\}^{-1} \tag{32}$$

The gravity anomaly at $r = R$ due to a spherical harmonic distribution of mass at the surface $r = R$ and at the Moho $r = R - b_c$ has been given by *Jeffreys* [1976, 5.06.2]. The result is

$$\Delta g_{cnm} = 4\pi G\left(\frac{n+1}{2n+1}\right)\left[\rho_c h_{cnm} - (\rho_m - \rho_c)\left(1 - \frac{b_c}{R}\right)^{n+2} w_{cnm}\right] \tag{33}$$

with a similar result for Δg_{snm}. Substitution of (26) into (33) gives

$$\Delta g_{cnm} = 4\pi G\left(\frac{n+1}{2n+1}\right)\rho_c h_{cnm}\left[1 - \left(1 - \frac{b_c}{R}\right)^{n+2} C_n\right] \tag{34}$$

In the limit of an infinitely rigid lithosphere $\tau \rightarrow \infty$ ($C_n \rightarrow 0$) this reduces to

$$\Delta g_{cnm\infty} = 4\pi G\left(\frac{n+1}{2n+1}\right)\rho_c h_{cnm} \tag{35}$$

Only the topography contributes to the surface free-air gravity anomaly since there is no deflection of the spherical shell and the Moho. In the limit of a lithosphere with no strength $\tau \rightarrow 0$, $\sigma \rightarrow 0$ ($C_n \rightarrow 1$) and (34) reduces to

$$\Delta g_{cnm0} = 4\pi G\left(\frac{n+1}{2n+1}\right)\rho_c h_{cnm}\left[1 - \left(1 - \frac{b_c}{R}\right)^{n+2}\right] \tag{36}$$

If $(1 - b_c/R)^{n+2} \simeq 1$, then $\Delta g_{cnm0} \simeq 0$, the result usually obtained for isostatic compensation of topography. We can also write

$$C_n = \frac{\Delta g_{nm\infty} - \Delta g_{nm}}{\Delta g_{nm\infty} - \Delta g_{nm0}} \tag{37}$$

which can be taken as a definition of the degree of compensation.

In order to compare with observations we wish to obtain the ratio of the gravitational potential anomaly due to topography to the height of the topography. The potential anomaly at $r = R$ due to a sperical harmonic distribution of mass at the surface $r = R$ and at the Moho $r = R - b_c$ from (22) is

$$\Delta U_{cnm} = -\frac{4\pi GR}{(2n+1)}\left[\rho_c h_{cnm} - (\rho_m - \rho_c)\left(1 - \frac{b_c}{R}\right)^{n+2} w_{cnm}\right] \tag{38}$$

And substitution of (26) gives

$$\Delta U_{cnm} = -\frac{4\pi GR\rho_c}{(2n+1)}\left[1 - \left(1 - \frac{b_c}{R}\right)^{n+2} C_n\right] h_{cnm} \tag{39}$$

TABLE 1. Planetary Properties Relating to the Present Value of the Stiffness Parameter τ_0

	Earth	Mars	Moon
Radius R, km	6378	3395	1738
Surface gravity g, cm/s^2	1000	380	165
Mean density $\bar{\rho}$, g/cm^3	5.517	3.94	3.34
Mass that contains radioactive isotopes, M_r, g	4.1×10^{27}	6.42×10^{26}	7.35×10^{25}
Thickness of the elastic lithosphere, d, km	50	90	207
τ_0	0.016	0.27	5.4
σ	8.74×10^{-8}	1.69×10^{-5}	6.81×10^{-3}

with a similar result for ΔU_{snm}. Since this result is independent of the order m it is often convenient to introduce a root mean square nondimensional nth degree gravity potential according to

$$\Delta U_n \equiv \frac{R}{GM} \sum_m (\Delta U_{cnm}{}^2 + \Delta U_{snm}{}^2)^{1/2} \tag{40}$$

and similarly for the topography

$$H_n \equiv \frac{1}{R} \sum_m (h_{cnm}{}^2 + h_{snm}{}^2)^{1/2} \tag{41}$$

And combining (39), (40), and (41) gives

$$\frac{\Delta U_n}{H_n} = \frac{3\rho_c}{(2n+1)\bar{\rho}} \left[1 - \left(1 - \frac{b_c}{R} \right)^{n+2} C_n \right] \tag{42}$$

This result will be compared with the observed ratios of gravitational potential to topography.

Application of the Harmonic Solution to the Moon and Mars

It is our object to determine whether membrane stresses support topographic and other loads on the earth, Mars, and the moon. In order to do this we first estimate the present value of τ for these planetary bodies. In all cases we take $E = 6.5 \times 10^{11}$ dyn/cm^2, $\nu = 0.25$, and $\rho_m - \rho_c = 0.5$ g/cm^3. The values of the radius R and the surface gravity g are given in Table 1. The major uncertainty involves the thickness of the elastic lithosphere d. For the earth based on a wide range of flexural problems [*Watts et al.*, 1980; *Caldwell and Turcotte*, 1979] it is estimated that the mean value of the elastic lithosphere is 50 ± 25 km. The base of the elastic lithosphere is believed to be defined by the temperature at which creep processes in the mantle rock relieve the elastic stress.

In order to estimate the present thickness of the elastic lithosphere on Mars and the moon it is assumed that the thickness is inversely proportional to the surface temperature gradient $d \sim (dT/dy)_0{}^{-1}$. In order to estimate the surface temperature gradient on Mars and the moon it is assumed that these bodies, as well as the earth, are in a steady state heat balance. The surface heat flow is attributed to the decay of radioactive isotopes. Further, it is assumed that the concentration of the radioactive isotopes on the three bodies is the same. The result is $(dT/dy)_0 \sim M_r/R^2$ where M_r is the mass in which the radioactive isotopes are distributed. For the earth M_r is taken to be the mass of the mantle and for Mars and the moon M_r is taken to be the mass of the entire body. Values are given in Table 1. The present thickness of the elastic lithospheres on Mars and the moon estimated from the relation $d \sim R^2/M_r$ and the value $d = 50$ km for the earth are also given in Table 1. The corresponding values of τ and σ are given. Because of the uncertainties in the thickness of the elastic lithosphere these values must be considered to be uncertain by at least a factor of 2. Nevertheless, several conclusions can be made. Membrane stresses on the earth do not support topographic loads. Membrane stresses on the moon are capable today of fully supporting topographic and other loads. On Mars membrane stresses can partially support topographic loads. In the past the thermal gradients and the thickness of the elastic lithosphere may have been considerably less than they are today. Regional variations can also be important. Therefore the values of τ_0 given in Table 1 should be considered only as estimates.

Earth

In order for membrane stresses to support topographic loads on the earth the elastic lithosphere would have to have a thickness of about 1000 km. There is no reason to believe that the earth ever had such a thick elastic lithosphere. It is therefore concluded that membrane stresses do not support topographic or other loads on the earth. However, the earth does have an ellipticity $\epsilon = 3.35 \times 10^{-3}$. When the surface plates change latitude due to continental drift their radius of curvature must change. As a result membrane stresses in the plates are generated [*Turcotte*, 1974]. These stresses do not, however, support topographic loads.

There is also strong evidence that topography and gravity on the earth are not correlated. The major topographic features are the continents. There are essentially no gravity anomalies associated with the continents. Major gravity anomalies such as the gravity low south of India have no topographic expressions. Therefore correlations of gravity and topography on the earth are unlikely to yield useful results.

Mars

We next consider Mars. Unlike the earth, topography and gravity on Mars are strongly correlated. The normalized coefficients for the gravitational potential have been given by *Christensen and Balmino* [1979]. The normalized coefficients for the topography have been given by *Bills and Ferrari* [1978]. Following *Lambeck* [1979] the ratios of the root mean square nth degree coefficients given by (40) and (41) are given

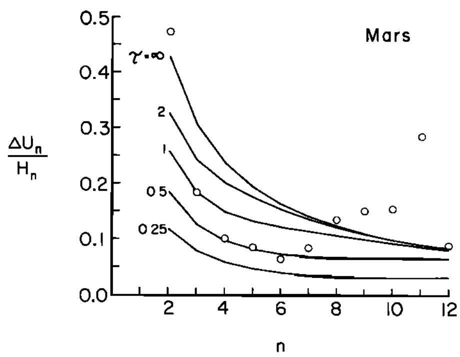

Fig. 1. Dependence of the ratio of the root mean square nth degree coefficients of gravitational potential and topography on the spherical harmonic degree n from (27) and (42) compared with the Martian data.

in Figure 1. Also included in Figure 1 are the predicted values for several values of τ from (42) and (27). For each value of τ the value of σ is obtained from (6) and (7). Taking $E = 6.5 \times 10^{11}$ dyn/cm^2, $\rho_m - \rho_c = 0.5$ g/cm^3 and R and g from Table 1 the thickness of the elastic lithosphere is determined from (6); then with $\nu = 0.25$ we determine σ from (7). Since the thickness of the crust on Mars is not known it is assumed that $b_c/R = 0$. As long as the Martian crust is thinner than 50 km the error introduced is less than 10% for degree 7 or less. In the range $n = 4$ to 7 the data correlate with $\tau \simeq 0.5$. The scattered values for $n = 8$ to 12 reflect the uncertainties in these coefficients. The value for $n = 2$ is undoubtedly related to rotation and is not relevant to our analysis.

We conclude $\tau = 0.5$ may be a good approximation for the rigidity of the Martian elastic lithosphere. The thickness of the elastic lithosphere corresponding to this value of τ is $h = 175$ km. It is seen from Table 1 that this is about twice the predicted value. There are several possible explanations for this factor of two difference. One is that the density difference that we have used between mantle and crust is too large. Another is that the extrapolation of the thermal gradient from the earth to Mars may be in error. Mars may have a lower concentration of radioactive isotopes or they may not be uniformly distributed.

It is of interest to determine the relative importance of bending and membrane stresses in supporting topographic loads on Mars. For $\tau = 0.5$ the value for σ from (7) is $\sigma = 1.09 \times 10^{-4}$. The corresponding values of C from (27) as a function of n are given in Figure 2. Also included in Figure 2 are the values of C obtained from (32) assuming $\tau = 0.5$ ($\sigma = 0$) and from (31) assuming $\sigma = 1.09 \times 10^{-4}$ ($\tau = 0$). We see that the load is primarily supported by membrane stresses for $n < 8$ and is primarily supported by bending stresses for $n > 8$. In the range $n = 4$–7 that we have been primarily interested in, membrane stresses dominate. The transition, $n = 8$, corresponds to a wavelength of 2700 km.

Moon

One of the surprising results from early lunar exploration was the large gravity anomalies associated with some lunar mare. These local gravity anomalies in excess of 200 mgal were attributed to mascons, regions of excess density beneath the lunar surface. It is clear that the lunar elastic lithosphere has been able to support this excess mass for more than 2×10^9 years. This support must be due to either bending or membrane stresses. Although we have shown that the present lunar elastic lithosphere is sufficiently thick so that membrane stresses can support the load of the mascons today, it is likely

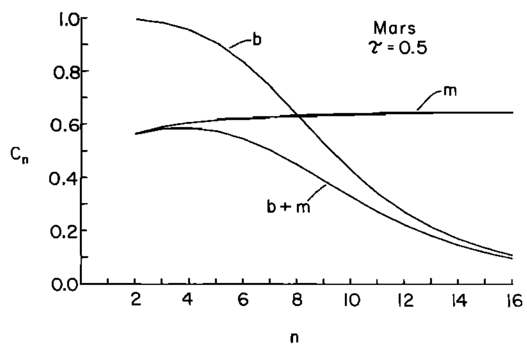

Fig. 2. Dependence of the degree of compensation C_n on n for Mars with $\tau = 0.5$: *b*, bending stresses only; *m*, membrane stresses only; *b* + *m*, bending and membrane stresses.

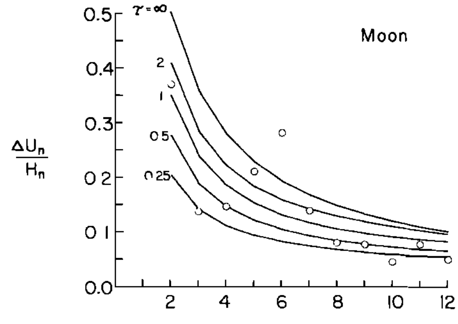

Fig. 3. Dependence of the ratio of the root mean square nth degree coefficients of gravitational potential and topography on the spherical harmonic degree n from (27) and (42) compared with the lunar data.

that the lunar lithosphere was thinner in the past. Since the rate of decay of radioactive isotopes was about twice the present value three billion years ago, the thickness of the elastic lithosphere may have been even less near the mascons at the time of their formation due to local heating.

Since the mascons are not the result of topographic loading their presence will interfere with any general correlation of gravity and topography on the moon. The normalized coefficients for the gravity potential to degree sixteen have been given by *Ferrari* [1977] and the topography coefficients to degree twelve have been given by *Bills and Ferrari* [1977]. These results are given in Figure 3. Also included in Figure 3 are the theoretical values from (42) and (27); the thickness of the lunar crust is taken to be 60 km. It is seen that there is considerable scatter although a number of the results lie close to the $\tau = 0.5$ result. The peak in the ratios of the coefficients near $n = 6$ is attributed to the mascons. The mascons have a positive gravity anomaly but no topography anomaly. This limited correlation with $\tau = 0.5$ can be attributed to the partial compensation of the lunar topography when it was being formed. For the moon $\tau = 0.5$ corresponds to a lunar elastic lithosphere with a thickness $h = 19.2$ km. This is not an unreasonable value if the topography was created early in the evolution of the moon.

We next determine the relative importance of bending and membrane stresses in supporting topographic loads on the moon. For $\tau = 0.5$ the corresponding value of $\sigma = 5.42 \times 10^{-6}$. The dependence of C_n on n from (27) is given in Figure 4. Also included in Figure 4 are the values of C_n obtained from (32) assuming $\tau = 0.5$ ($\sigma = 0$) and from (31) assuming $\sigma = 5.42 \times 10^{-6}$ ($\tau = 0$). We see that the load is primarily supported by membrane stresses if $n < 17$ and is primarily supported by bending stresses if $n > 17$. The transition, $n = 17$, corresponds to a wavelength of 642 km.

The mascons are not the only features on the moon associated with large free-air gravity anomalies. The Appennine Mountains on the moon are a region elevated topography with an amplitude of about 2 km and a horizontal extent of several hundred kilometers. It has been argued by *Ferrari et al.* [1978] that the Appennines are not compensated. We suggest that the topography of the Appennines has been supported by membrane stresses for some three billion years.

VARIATION OF PARAMETERS

We have shown that topographic loads on the moon are primarily supported by membrane stresses if their horizontal

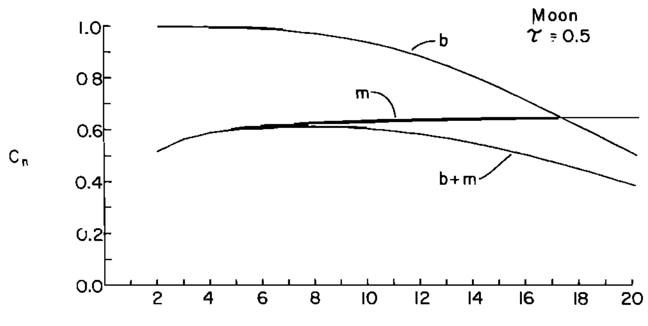

Fig. 4. Dependence of the degree of compensation C_n on n for the moon with $\tau = 0.5$: b, bending stresses only; m, membrane stresses only; $b + m$, bending and membrane stresses.

extent is greater than about 320 km (half the wavelength) and on Mars if their horizontal extent is greater than about 1300 km. Although the harmonic analysis provides useful results, it is difficult to apply it to localized loads. In this section we will obtain an analytic solution for the surface displacement and stress field for an axisymmetric load ($\partial/\partial\psi = 0$) assuming membrane stresses support the load. We will also assume the horizontal extent of the load is relatively small so that $h_g \simeq 0$ and $\bar{h} \simeq h$.

Assuming $\sigma = 0$, $\partial/\partial\psi = 0$ and $\bar{h} = h$, (8) and (2) simplify to give

$$\left[\frac{\partial^2}{\partial\phi^2} + \cot\phi\frac{\partial}{\partial\phi} + \left(\frac{1-\nu+2\tau}{1+\tau}\right)\right]w = \frac{\rho_c}{(\rho_m-\rho_c)(1+\tau)}\left(\frac{\partial^2}{\partial\phi^2} + \cot\frac{\partial}{\partial\phi} + 1 - \nu\right)h \tag{43}$$

Introducing (15) as well as

$$z = w - \left(\frac{\rho_c}{\rho_m-\rho_c}\right)\frac{h}{(1+\tau)} \tag{44}$$

$$a = \left(\frac{\rho_c}{\rho_m-\rho_c}\right)\frac{\tau(1+\nu)}{(1+\tau)^2} \tag{45}$$

$$s(s+1) = \frac{1-\nu+2\tau}{1+\tau} \tag{46}$$

substitution into (43) yields

$$(1-\xi^2)\frac{d^2z}{d\xi^2} - 2\xi\frac{dz}{d\xi} + s(s+1)z = -ah \tag{47}$$

The left side of (47) is Legendre's equation of degree s and order 0. In the limit $\tau \to \infty$, $s \to 1$. In the limit $\tau = 0$, $s = -\frac{1}{2} + \frac{1}{2}[1 + 4(1-\nu)]^{1/2}$. A typical value of ν for the lithosphere is 1/4 and for this case $s = 1/2$.

Two independent solutions of the homogeneous Legendre's equation are the Legendre functions $P_s(\xi)$ and $Q_s(\xi)$. The values of $P_s(\xi)$ for fractional degree have been tabulated by *Gray* [1953]; $Q_s(\xi)$ can then be obtained from the relation

$$Q_s(\xi) = \frac{\pi}{2\sin(s\pi)}[\cos(s\pi)P_s(\xi) - P_s(-\xi)] \tag{48}$$

We now obtain a general solution of the inhomogeneous Legendre's equation, (38), using the method of variation of parameters.

A solution of (48) is written in the form

$$z = A(\xi)P_s(\xi) + B(\xi)\left[Q_s(\xi) - \frac{\pi}{2}\cot(s\pi)P_s(\xi)\right] \tag{49}$$

where $A(\xi)$ and $B(\xi)$ are unknown functions that must be determined. The range of ξ is $-1 < \xi < 1$; $P(\xi)$ is singular at $\xi = -1$ and $Q_s(\xi)$ is singular at $\xi = \pm 1$. In order to examine these singularities we give the asymptotic forms of $P_s(\xi)$ and $Q_s(\xi)$ near $\xi = \pm 1$ [*Erdelyi*, 1953]

as $\xi \to 1$:

$$P_s(\xi) \to 1 \tag{50}$$

$$Q_s(\xi) \to -\frac{1}{2}\ln\left|\frac{1}{2} - \frac{1}{2}\xi\right| - \frac{1}{2}\gamma - \psi(s+1) \tag{51}$$

$$Q_s(\xi) - \frac{\pi}{2}\cot(s\pi)P_s(\xi) \to -\frac{1}{2}\ln\left|\frac{1}{2} - \frac{1}{2}\xi\right| - \frac{1}{2}\gamma - \psi(s+1) - \frac{\pi}{2}\cot(s\pi) \tag{52}$$

as $\xi \to -1$:

$$P_s(\xi) \to \frac{\sin(s\pi)}{\pi}\left[\ln\left|\frac{1}{2} + \frac{1}{2}\xi\right| + \gamma + 2\psi(s+1) + \pi\cot(s\pi)\right] \tag{53}$$

$$Q_s(\xi) \to \frac{\cos(s\pi)}{2}\left[\ln\left|\frac{1}{2} + \frac{1}{2}\xi\right| + \gamma + 2\psi(s+1) - \pi\tan(s\pi)\right] \tag{54}$$

$$Q_s(\xi) - \frac{\pi}{2}\cot(s\pi)P_s(\xi) \to -\frac{\pi}{2\sin(s\pi)} \tag{55}$$

where $\gamma = 0.577$ is Euler's constant and $\psi(s+1)$ is the logarithmic derivative of the gamma function [*Abramowitz and Stegun*, 1965]. The reason that the combination $Q_s(\xi) - (\pi/2)\cot(s\pi)P_s(\xi)$ was introduced in (49) was to avoid the singular behavior of $P_s(-1)$ and $Q_s(-1)$ as shown in (55). The combination is not singular at $\xi = -1$.

We next take the derivative of (49) with respect to ξ with the result

$$\frac{dz}{d\xi} = \left[\frac{dA}{d\xi} - \frac{\pi}{2}\cot(s\pi)\frac{dB}{d\xi}\right]P_s + \frac{dB}{d\xi}Q_s + \left[A - \frac{\pi}{2}\cot(s\pi)B\right]\frac{dP_s}{d\xi} + B\frac{dQ_s}{d\xi} \tag{56}$$

We require that

$$\left[\frac{dA}{d\xi} - \frac{\pi}{2}\cot(s\pi)\frac{dB}{d\xi}\right]P_s + \frac{dB}{d\xi}Q_s = 0 \tag{57}$$

so that (56) reduces to

$$\frac{dz}{d\xi} = \left[A - \frac{\pi}{2}\cot(s\pi)B\right]\frac{dP_s}{d\xi} + B\frac{dQ_s}{d\xi} \tag{58}$$

Again taking the derivative of (58) with respect to ξ gives

$$\frac{d^2z}{d\xi^2} = \left[\frac{dA}{d\xi} - \frac{\pi}{2}\cot(s\pi)\frac{dB}{d\xi}\right]\frac{dP_s}{d\xi} + \frac{dB}{d\xi}\frac{dQ_s}{d\xi} + \left[A - \frac{\pi}{2}\cot(s\pi)B\right]\frac{d^2P_s}{d\xi^2} + B\frac{d^2Q_s}{d\xi^2} \qquad (59)$$

Substituting (58) and (59) into (47) noting that

$$(1-\xi^2)\frac{d^2P_s}{d\xi^2} - 2\xi\frac{dP_s}{d\xi} + s(s+1)P_s = 0 \qquad (60)$$

$$(1-\xi^2)\frac{d^2Q_s}{d\xi^2} - 2\xi\frac{dQ_s}{d\xi} + s(s+1)Q_s = 0 \qquad (61)$$

gives

$$(1-\xi^2)\left\{\left[\frac{dA}{d\xi} - \frac{\pi}{2}\cot(s\pi)\frac{dB}{d\xi}\right]\frac{dP_s}{d\xi} + \frac{dB}{d\xi}\frac{dQ_s}{d\xi}\right\} = -ah \qquad (62)$$

Eliminating $dA/d\xi$ from (57) and (62) gives

$$\frac{dB}{d\xi} = \frac{P_s ah}{(1-\xi^2)[Q_s(dP_s/d\xi) - P_s(dQ_s/d\xi)]} \qquad (63)$$

The Wronskian of the orthogonal functions P_s and Q_s is defined as [*Abramowitz and Stegun*, 1965]

$$w[P_s(\xi), Q_s(\xi)] \equiv P_s\frac{dQ_s}{d\xi} - Q_s\frac{dP_s}{d\xi} = \frac{1}{1-\xi^2} \qquad (64)$$

Substitution of (64) into (63) gives

$$\frac{dB}{d\xi} = -aP_s h \qquad (65)$$

and this is integrated to give

$$B = a\int_\xi^1 P_s(\xi')h(\xi')\,d\xi' \qquad (66)$$

The solution for z in (49) must not be singular at $\xi = 1$. Since from (57) $Q_s(\xi)$ is singular as $\xi \rightarrow 1$ it is necessary that $B(1) = 0$. This condition requires that the upper limit of the integral in (66) be $+1$.

Eliminating $dB/d\xi$ from (57) and (62) gives

$$\frac{dA}{d\xi} = \frac{[Q_s - (\pi/2)\cot(s\pi)\,P_s]ah}{(1-\xi^2)[P_s(dQ_s/d\xi) - Q_s(dP_s/d\xi)]} \qquad (67)$$

Substitution of (64) yields

$$\frac{dA}{d\xi} = \left[Q_s - \frac{\pi}{2}\cot(s\pi)\,P_s\right]ah \qquad (68)$$

And this is integrated to give

$$A = a\int_{-1}^{\xi}\left[Q_s(\xi') - \frac{\pi}{2}\cot(s\pi)P_s(\xi')\right]h(\xi')\,d\xi' \qquad (69)$$

The solution for z in (49) must also not be singular at $\xi = -1$. Since from (53) $P_s(\xi)$ is singular as $\xi \rightarrow -1$ it is necessary that $A(-1) = 0$. This condition requires that the lower limit of the integral in (69) be -1. Substitution of (66) and (69) into (49) gives

$$z = aP_s(\xi)\int_{-1}^{\xi}\left[Q_s(\xi') - \frac{\pi}{2}\cot(s\pi)P_s(\xi')\right]h(\xi')\,d\xi' + a\left[Q_s(\xi) - \frac{\pi}{2}\cot(s\pi)P_s(\xi)\right]\int_\xi^1 P_s(\xi')h(\xi')\,d\xi' \qquad (70)$$

When the topography $h(\xi)$ has been specified the displacement w can be obtained from (44) and (70). A numerical integration is required.

In many cases a topographic load is applied over a small fraction of the planetary body. If the load is applied in the region $\phi < \phi_0$ with $\phi_0 \ll 1$ it is possible to considerably simplify (70). The asymptotic forms of $P_s(\xi)$ and $Q_s(\xi)$ from (52) and (53) can be used in evaluating the integrals. Making the appropriate approximations in (70) and combining them with (44) and (45), we obtain

$$w = \left(\frac{\rho_c}{\rho_m - \rho_c}\right)\frac{1}{(1+\tau)}\left[h + \frac{\tau(1+\nu)}{(1+\tau)}\left\{P_s(\cos\phi)\cdot\int_\phi^\infty\left[-\frac{1}{2}\ln\phi' - \frac{1}{2}\gamma - \psi(s+1) - \frac{\pi}{2}\cot(s\pi)\right]h(\phi')\phi'\,d\phi' + \left[Q_s(\cos\phi) - \frac{\pi}{2}\cot(s\pi)P_s(\cos\phi)\right]\int_0^\phi h(\phi')\phi'\,d\phi'\right\}\right] \qquad (71)$$

As a specific example we assume that

$$h = h_0 e^{-(\phi/\phi_0)^2} \qquad (72)$$

with $\phi_0 \ll 1$. We wish to determine w_0, the amplitude of w at $\phi = 0$. Substitution of (72) into (71) with $\phi = 0$ yields

$$w_0 = \left(\frac{\rho_c}{\rho_m - \rho_c}\right)\frac{1}{(1+\tau)}\left[h_0 + \frac{\tau(1+\nu)}{(1+\tau)}\int_0^\infty\left[-\frac{1}{2}\ln\phi' - \frac{1}{2}\gamma - \psi(s+1) - \frac{\pi}{2}\cot(s\pi)\right]h_0 e^{-(\phi'/\phi_0)^2}\phi'\,d\phi'\right] \qquad (73)$$

Noting that ϕ_0 is small the leading terms after integration are

$$w_0 = \left(\frac{\rho_c}{\rho_m - \rho_c}\right)\frac{h_0}{(1+\tau)}\left[1 - \frac{\tau(1+\nu)}{8(1+\tau)}\phi_0^2\ln\phi_0^2\right] \qquad (74)$$

And neglecting the second term the general result is obtained that

$$w = \left(\frac{\rho_c}{\rho_m - \rho_c}\right)\frac{h}{(1+\tau)} \qquad (75)$$

Introducing the definition of the degree of compensation C_n from (26), we obtain

$$C = \frac{1}{1+\tau} \qquad (76)$$

This result is also obtained from (32) in the limit $n \rightarrow \infty$. This simple result is valid for intermediate values of n, n large compared with unity but sufficiently small that membrane stresses support the topographic load.

We next derive expressions for the distribution of membrane stress. The two components of membrane stress are related to the pressure on the shell by [*Turcotte,* 1974]

$$\sigma_\phi + \sigma_\psi = \frac{R}{d} p \tag{77}$$

$$\frac{d}{d\phi}[(\sin \phi)\sigma_\phi] = (\cos \phi)\, \sigma_\psi \tag{78}$$

Elimination of σ_ψ gives

$$\frac{d\sigma_\phi}{d\phi} + 2(\cot \phi)\sigma_\phi = \frac{R}{d}(\cot \phi)\, p \tag{79}$$

Integration of this first-order differential equation using an integration factor yields

$$\sigma_\phi = \frac{R}{d \sin^2 \phi} \int_0^\phi \sin \phi' \cos \phi' p(\phi')\, d\phi' \tag{80}$$

The constant of integration has been set equal to zero in order to avoid singular behavior at $\phi = 0$. Substitution of (80) into (77) gives

$$\phi_\psi = \frac{R}{d}\left[p(\phi) - \frac{1}{\sin^2 \phi} \int_0^\phi \sin \phi' \cos \phi' p(\phi')\, d\phi'\right] \tag{81}$$

As a specific example we consider the topographic load given in (72). Substitution of (72) and (75) into (3) with $h_g = 0$ gives

$$p = \left(\frac{\tau}{1+\tau}\right) g\rho_c h_0 e^{-(\phi/\phi_0)^2} \tag{82}$$

Substitution of (82) into (80) and (81) yields

$$\bar{\sigma}_\phi \equiv \frac{d(1+\tau)\sigma_\phi}{R\tau\rho_c g h} = \frac{1}{2}\left(\frac{\phi_0}{\phi}\right)^2 [1 - e^{-(\phi/\phi_0)^2}] \tag{83}$$

$$\bar{\sigma}_\psi = \frac{d(1+\tau)\sigma_\psi}{R\tau\rho_c g h} = e^{-(\phi/\phi_0)^2} - \frac{1}{2}\left(\frac{\phi_0}{\phi}\right)^2 (1 - e^{-(\phi/\phi_0)^2}) \tag{84}$$

The dependence of the two components of the nondimensional membrane stress on position is given in Figure 5. The polar component σ_ϕ is always positive (compressional) but the azimuthal component σ_ψ is positive (compressional) for $0 < \phi < 1.12\phi_0$ and negative (tensional) for $\phi > 1.12\phi_0$. At the transition point $h/h_0 = 0.326$. The maximum value of the tensional azimuthal stress is $\bar{\sigma}_\psi = -0.108$ and it occurs at $\phi/\phi_0 = 1.73$.

Application of the Variation of Parameters Solution to Mars

We will apply the variation of parameters solution to the problem of the support of the Tharsis region on Mars. *Bills and Ferrari* [1978] have concluded that $C = 0.6$–0.65 for the Tharsis region. From (76) this gives $\tau = 0.54$–0.67; this is in good agreement with the value $\tau = 0.5$ obtained from the harmonic analysis and the spectral correlation of the observed gravitational potential and topography.

We further assume that the topography of the Tharsis region can be represented by (72) taking $h_0 = 10$ km and $\phi_0 = 30°$. The width of the load is therefore 60° or 3550 km. If this is associated with the wavelength of a spherical harmonic it corresponds to $n = 6$. As seen from Figure 4 this is in the range of n in which membrane stresses dominate over bending stresses. If we take $\rho_c = 2.8$ g/cm³, $\tau = 0.54$, and $d = 180$ km the maximum stress at the center of the load from (65) is 3.5

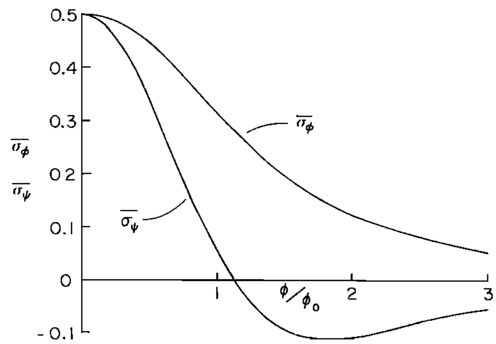

Fig. 5. Dependence of the nondimensional membrane stress components from (83) and (84) on the angular distance from the center of the load.

kbar. With $\phi_0 = 30°$ the azimuthal stress is tensional at distances greater than 1990 km from the center of the load. The maximum value of the tensional stress is $\sigma_\psi = -750$ bars and it occurs 3075 km from the center of the load. The tensional azimuthal membrane stresses surrounding Tharsis may be an explanation for the extensive radial fracturing observed in that area.

Conclusions

We conclude that membrane stresses play an important role in the support of topographic loads on the moon and Mars. The correlation of observed gravitational potential anomalies with topography on Mars is explained by membrane stresses in the elastic lithosphere. These stresses can explain the unexpected large gravity anomaly associated with the Tharsis uplift. The tensional, azimuthal membrane stresses are likely to be responsible for the extensive set of radial fractures surrounding much of the Tharsis region.

The strong gravity anomalies associated with the mascons on the moon mask any systematic correlation of the observed gravitational potential anomalies with topography. Nevertheless, we expect membrane stresses to play an important role in the support of topographic loads on the moon.

Acknowledgments. Participation in the Tharsis working group sponsored by the Jet Propulsion Laboratory with Roger Phillips as chairman stimulated our interest in these problems. We would like to acknowledge many stimulating discussions with Roger as well as Norman Sleep and Sean Solomon. This research was sponsored by the National Aeronautics and Space Administration under grant NGR-33-010-108 and is contribution 685 of the Department of Geological Sciences, Cornell University.

References

Abramowitz, M., and I. A. Stegun, *Handbook of Mathematical Functions,* Dover, New York, 1965.

Banks, R. J., and C. J. Swain, The isostatic compensation of East Africa, *Proc. R. Soc. London, Ser. A, 364,* 331–352, 1978.

Banks, R. J., R. L. Parker, and S. P. Huestis, Isostatic compensation on a continental scale: Local versus regional mechanisms, *Geophys. J. R. Astron. Soc., 51,* 431–452, 1977.

Bills, B. G., and A. J. Ferrari, A harmonic analysis of lunar topography, *Icarus, 31,* 244–259, 1977.

Bills, B. G., and A. J. Ferrari, Mars topography harmonics and geophysical implications, *J. Geophys. Res., 83,* 3497–3508, 1978.

Caldwell, J. G., and D. L. Turcotte, Dependence of the thickness of the elastic oceanic lithosphere on age, *J. Geophys. Res., 84,* 7572–7576, 1979.

Christensen, E. T., and G. Balmino, Analysis of a twelfth degree and order gravity model for Mars, *J. Geophys. Res., 84,* 7943–7953, 1979.

Dorman, L. M., and B. T. R. Lewis, Experimental isostasy, 3, Inversion of the isostatic Green's function and lateral density changes, *J. Geophys. Res.*, *77*, 3068–3077, 1972.

Erdelyi, A., *Higher Transcendental Functions*, vol. 1, pp. 120–181, McGraw-Hill, New York, 1953.

Ferrari, A. J., Lunar gravity: A harmonic analysis, *J. Geophys. Res.*, *82*, 3065–3084, 1977.

Ferrari, A. J., D. L. Nelson, W. L. Sjogren, and R. J. Phillips, The isostatic state of the lunar Apennines and regional surroundings, *J. Geophys. Res.*, *83*, 2863–2871, 1978.

Gray, M. C., Legendre functions of fractional order, *Q. Appl. Math.*, *11*, 311–318, 1953.

Jeffreys, H., *The Earth*, 6th ed., Cambridge University Press, New York, 1976.

Kraus, H., *Thin Elastic Shells*, John Wiley, New York, 1967.

Lambeck, K., Comments on the gravity and topography of Mars, *J. Geophys. Res.*, *84*, 6241–6247, 1979.

McNutt, M. K., and R. L. Parker, Isostasy in Australia and the evolution of the compensation mechanism, *Science*, *199*, 773–775, 1978.

Sjogren, W. L., Lunar gravity determinations and their implications, *Philos. Trans. R. Soc. London, Sect. A*, *285*, 219–226, 1977.

Turcotte, D. L., Membrane tectonics, *Geophys. J. R. Astron. Soc.*, *36*, 33–42, 1974.

Watts, A. B., J. H. Bodine, and N. M. Ribe, Observations of flexure and the geological evolution of the Pacific Ocean basin, *Nature*, *283*, 532–537, 1980.

(Received June 19, 1980;
revised December 1, 1980;
accepted December 31, 1980.)